Organic Photoswitches Hot Paper

How to cite: *Angew. Chem. Int. Ed.* **2022,** *61,* e202117158
International Edition: doi.org/10.1002/anie.202117158
German Edition: doi.org/10.1002/ange.202117158

Reversible Three-Color Fluorescence Switching of an Organic Molecule in the Solid State via "Pump–Trigger" Optical Manipulation

Runqing Yang[+], Xue Ren[+], Lijun Mei, Guocui Pan, Xiao-Ze Li, Zhiyuan Wu, Song Zhang, Wenyue Ma, Weili Yu, Hong-Hua Fang, Chong Li, Ming-Qiang Zhu, Zheng Hu, Tianmeng Sun, Bin Xu, and Wenjing Tian*

Abstract: In photoswitches that undergo fluorescence switching upon ultraviolet irradiation, photoluminescence and photoisomerization often occur simultaneously, leading to unstable fluorescence properties. Here, we successfully demonstrated reversible solid-state triple fluorescence switching through "Pump–Trigger" multiphoton manipulation. A novel fluorescence photoswitch, BOSA-SP, achieved green, yellow, and red fluorescence under excitation by pump light and isomerization induced by trigger light. The energy ranges of photoexcitation and photoisomerization did not overlap, enabling appropriate selection of the multiphoton light for "pump" and "trigger" photoswitching, respectively. Additionally, the large free volume of the spiropyran (SP) moiety in the solid state promoted reversible photoisomerization. Switching between "pump" and "trigger" light is useful for three-color tunable switching cell imaging, which can be exploited in programmable fluorescence switching. Furthermore, we exploited reversible dual-fluorescence switching in a single molecular system to successfully achieve two-color super-resolution imaging.

Introduction

Solid-state fluorescence photoswitches that can change their fluorescence color in response to remote light have received considerable interest because of their various applications in optoelectronic devices,[1] information storage,[2] and biological imaging.[3] Recently, the modification of various fluorescent groups on classic photoisomerizable moieties, such as spiropyran (SP),[2a,b,4] dithienylethene,[5] and fulgide,[2d,6] has enabled the development of a variety of solid-state photofluorochromic materials. Traditionally, SP can change from a closed orthogonal form to an open conjugated zwitterionic merocyanine (MC) under excitation by light. However, this transition is accompanied by a noticeable change, namely, red fluorescence.[7] Nonetheless, the photoisomerized SP can be reversibly recovered under stimulation with heat or visible light.[8] Photoswitches in which SP is modified with different fluorogens exhibit novel dual photofluorochromic properties in the aggregated state and have versatile applications in several areas, such as anti-counterfeiting[2b,c,4a,d] and super-resolution imaging.[2b,3d] Generally, short-wavelength light ($\lambda < 420$ nm) is used to induce photoluminescence and photoisomerization in SP-based solid-state photoswitches. However, photoisomerization of the SP moiety in photoswitches is highly sensitive to short-wavelength light,[9] where the molecular structure of the SP-based photoswitches changes rapidly under irradiation with

[*] R. Yang,[+] X. Ren,[+] G. Pan, Z. Wu, S. Zhang, W. Ma, Prof. B. Xu, W. Tian
State Key Laboratory of Supramolecular Structure and Materials, College of Chemistry, Jilin University
Qianjin Street No. 2699, Changchun 130012 (China)
E-mail: xubin@jlu.edu.cn

X. Ren[+]
Department of Oncological Gynecology, The First Hospital of Jilin University
Changchun 130012 (China)

Prof. Z. Hu, Prof. T. Sun
Key Laboratory of Organ Regeneration & Transplantation of Ministry of Education, The First Hospital of Jilin University
Changchun 130061 (China)

L. Mei, Prof. C. Li, Prof. M.-Q. Zhu
Wuhan National Laboratory for Optoelectronics (WNLO), School of Optics and Electronic Information, Huazhong University of Science and Technology
Wuhan 430074 (China)

Prof. W. Yu
GPL Photonic Laboratory, State Key Laboratory of Applied Optics, Changchun Institute of Optics, Fine Mechanics and Physics, Chinese Academy of Sciences
Changchun 130033 (China)

X.-Z. Li, Prof. H.-H. Fang
State Key Laboratory of Precision Measurement Technology & Instruments, Department of Precision Instrument, Tsinghua University
Beijing 100084 (China)

[+] These authors contributed equally to this work.

single short-wavelength light. Scheme 1a shows that such changes inevitably cause the initial fluorescence from the fluorogen moiety of the SP-based photoswitches to quickly switch to the red fluorescence of the MC moiety either via intramolecular energy transfer or charge transfer. However, the initial fluorescence cannot be stably identified,[10] which limits the practical applications of these photoswitches. Selective and stable output of fluorescence signals can be achieved if the properties of solid-state photoswitches are controlled and interference from photoluminescence and photoisomerization are avoided.

In this study, the "Pump–Trigger" strategy is used to demonstrate reversible solid-state fluorescence switching. It has been reported that short-wavelength light ($\lambda < 420$ nm) can be used to achieve photoisomerization between SP and MC through a one-photon process, while near-infrared (NIR) light (780–840 nm) can be used to achieve photoisomerization through a two-photon process.[3c,11] Thus, the wavelength range of 420–780 nm is suitable as "pump" light for the photoluminescence of the fluorogen moiety without inducing photoisomerization of the SP moiety, and UV light ($\lambda < 420$ nm) or NIR light (780–840 nm) can act as "trigger" light to regulate photoisomerization of the solid-state photoswitches. More importantly, the alternate use of "pump" light and "trigger" light can possibly enable control of the fluorescence switching of solid-state photoswitches.

To achieve the fluorescence switching, the fluorogen moiety of the SP-based photoswitch should be judiciously selected. Ideally, the moiety should efficiently emit one-photon fluorescence (OPF) under excitation with visible light (420–780 nm) and two-photon fluorescence (TPF) under excitation with NIR light. By compared with the well-known AIEgens TPE,[12a,b] DSA and its derivatives could not only provide more suitable excitation bands that extending to visible light (one-photon process) or NIR light (two-photon processes), but also possess excellent AIE characteristics which can obtain highly emission in aggregate state.[12c–g] Specifically, we develop a novel solid-state fluorescence photoswitch, BOSA-SP by connecting DSA derivatives, BOSA, with SP in a one-to-one ratio through a flexible covalent ester chain. Programmable triple fluorescence switching characteristics of BOSA-SP can be achieved as follows under stimulation with "pump" light and "trigger" light, respectively: 1) under irradiation with "pump" light (488/950 nm), BOSA-SP can stably emit green fluorescence in the solid state; 2) under irradiation with "trigger" light (365/405 nm), BOSA-SP can change to BOSA-MC. This transformation is accompanied by a transition from green to red fluorescence and the reverse-"trigger" light (524 nm) can cause BOSA-MC to revert to BOSA-SP; 3) under special irradiation with "pump" light (800 nm), BOSA-SP in the solid state emits dramatic yellow TPF, which is the superposition of green fluorescence and red fluorescence; 4) continuous light (800 nm) can also act as a "trigger" to transform BOSA-SP into BOSA-MC. This transformation is accompanied by a shift from yellow to red fluorescence, and the reverse-"trigger" light (524 nm) can cause BOSA-MC to revert to BOSA-SP in the solid state (Scheme 1b). Owing to these controllable solid-state triple fluorescence switching properties, BOSA-SP prospectively has multiple applications in various fields, such as three-color tunable switching cellular imaging and two-color super-resolution imaging.

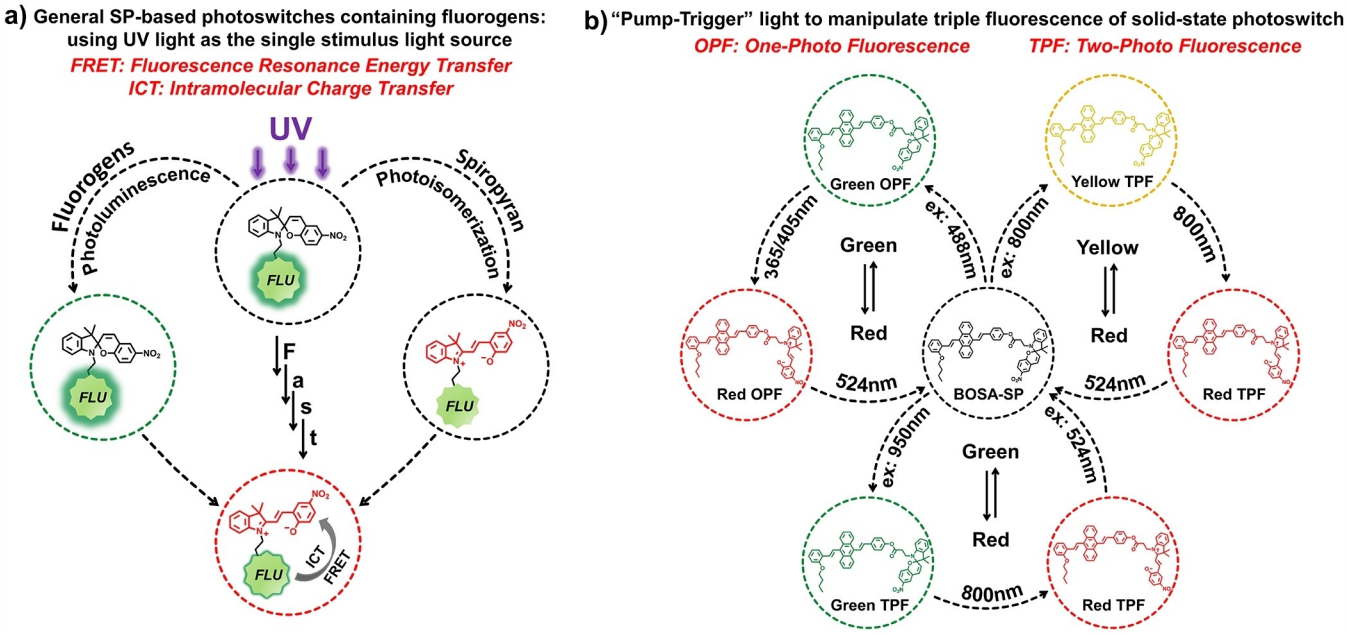

Scheme 1. a) Schematic illustrating fast fluorescence switching of general SP-based solid-state fluorescence photoswitches under UV-light irradiation. b) Schematic of controllable triple fluorescence switching of the solid-state photoswitch, BOSA-SP, with multi-waveband light.

Results and Discussion

Synthesis and Characterization of BOSA-SP

Similar to the reported procedure, BOSA-SP was synthesized by an esterification reaction in which BOSA (DSA derivative) was connected to SP. The synthesis of BOSA-SP is shown in Schemes S1–S4. ^{1}H NMR spectroscopy and high-resolution mass spectroscopy (HRMS) were used to characterize all the compounds.

Controllable Triple Fluorescence Switching

We first studied the photophysical properties of the BOSA-SP powders upon photoirradiation (Figure 1a). Figures 1b and d show that before ultraviolet (UV) irradiation, the BOSA-SP powders were yellow during daylight and emitted bright green fluorescence under excitation with 365 nm UV light. The resultant spectra evidenced that the powdered BOSA-SP absorbed UV light with a λ_{max} peak at 416 nm and an emission peak centered at 532 nm, which may be attributed to the BOSA moiety. Under continuous 365 nm (UV) irradiation, the color of the powders turned purple-black (Video 1), as evidenced by a new absorption band (λ_{max} = 576 nm), and the fluorescence of the powders changed from green (532 nm) to red (692 nm) (Figure S1). Detailed time-dependent spectroscopy studies showed that under continuous UV-light irradiation, the intensity of the new absorption (576 nm) and emission peaks (692 nm) gradually intensified, and the emission peak centered at 532 nm gradually declined (Figures 1c and d). These results indicate that UV light successfully triggered the switch from BOSA-SP to BOSA-MC in the solid state (Figure 1a).[2b,c] And the absorbance of BOSA-MC solid film dropped less after 48 hours of non-stop testing in a dark environment (Figure S2). This result demonstrates that BOSA-MC exhibited good stability in the solid state. Additionally, the color and fluorescence of the BOSA-MC powders could be restored to their original state under irradiation with 524 nm light (Figure 1b, S1, and Video 2). Time-dependent spectroscopy (Figures 1e and f) showed that the intensity of the absorption band (576 nm) and emission peak (692 nm) decreased to the initial state after approximately 3 h of continuous irradiation with 524 nm light, which further verified that 524 nm light can effectively trigger the reversal of BOSA-MC to BOSA-SP in the solid state. This preliminary test revealed that BOSA-SP in the aggregated state exhibited reversible fluorescent photoswitching properties under an alternating trigger of 365 nm light and 524 nm light. The reversible absorption and emission photoresponses of BOSA-SP were evaluated over several cycles, proving that BOSA-SP exhibits good fatigue resistance (Figure S3).

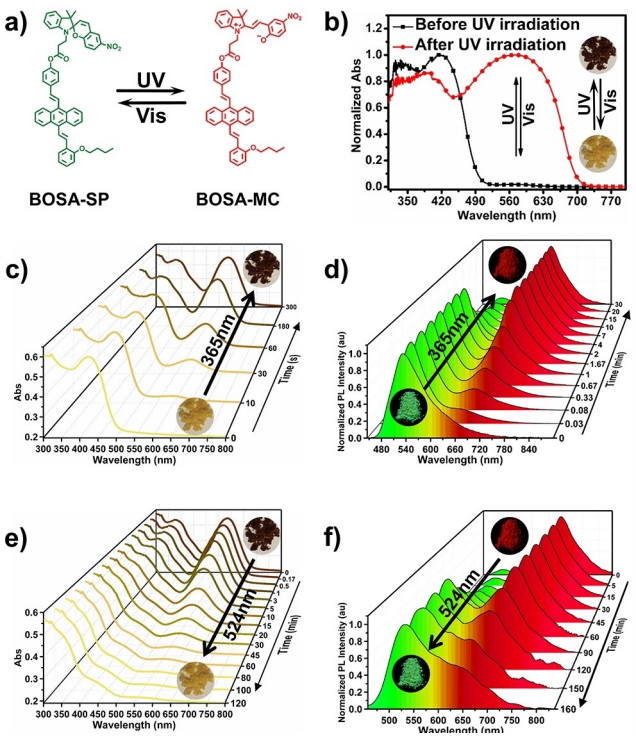

Figure 1. a) Reversible structure isomerization of BOSA-SP and BOSA-MC. b) UV/Vis absorption spectra of BOSA-SP powders before and after UV irradiation. The inset shows visible images of the BOSA-SP powders before and after UV irradiation. Irradiation time-dependent c) absorbance and d) PL spectra recorded for BOSA-SP powders upon irradiation with 365 nm light (12.15 mW cm^{-2}). Irradiation time-dependent e) absorbance and f) PL spectra recorded for BOSA-MC powders upon irradiation with 524 nm light (18.54 mW cm^{-2}). The inset shows the visible and fluorescence images of the BOSA-SP and BOSA-MC powders.

The reversible fluorescence switching of BOSA-SP encouraged us to further explore manipulation of the photoisomerization of SP-based solid-state photoswitches. As aforementioned, the non-overlapping waveband (420–780 nm) is very suitable as "pump" light to steadily excite the fluorogen moiety and induce photoluminescence without causing photoisomerization of the SP moiety. Figure S4a shows that under the excitation with 488 nm light, the BOSA-SP powders exhibited emission peaks at 540 nm and 695 nm before and after irradiation with UV light, respectively, which confirmed that 488 nm light was appropriate for fluorescence excitation. In order to verify the effectiveness and stability of 488 nm light as the "pump" light, the time-dependence of the fluorescence intensity at 540 nm and 692 nm was evaluated for the BOSA-SP powders after continuous excitation with 488 nm light (Figure S4b). After 12 min of continuous excitation with 488 nm light (6.21 mW cm^{-2}), the fluorescence intensity of BOSA-SP at 540 nm only declined by 8 %, and almost no fluorescence was detected at 692 nm, which suggests that the SP moiety was ineffectively photoisomerized. Comparatively, BOSA-SP steadily emitted green fluorescence under continuous irradiation with "pump" light (488 nm). The pump light (488 nm) was then switched to the trigger light (405 nm, 7.35 mW cm^{-2}) (Figure S4b). Notably, decreased (540 nm) and increased (692 nm) fluorescence were observed under irradiation with 405 nm light for several minutes before a photostationary state was reached. Therefore, after excita-

tion by the "pump" light (488 nm), the fluorescence of excited BOSA-SP can be selectively switched between green and red under the action of the "trigger" light (365/405/524 nm).

As aforementioned, "pump" light (488 nm) and "trigger" light (365/405/524 nm) were successfully used to achieve the one-photon induced reversible solid-state dual-fluorescence switching (green-red) of BOSA-SP (Figure 2a). Based on the two photon-induced photoisomerization of SP and photoluminescence of DSA derivatives,[11c,12c,g] we studied the photophysical properties of BOSA-SP powders upon irradiation with 800 nm NIR femtosecond laser light. In contrast to the green fluorescence produced after the BOSA-SP powders were excited with "pump" light (488 nm), the BOSA-SP powders exhibited a particular yellow fluorescence under excitation of NIR "Pump light" (800 nm), which originated from the two-photon process. The corresponding fluorescence spectrum shows peaks at 526 nm and 671 nm (Figure 2b), corresponding to the production of yellow fluorescence with coordinates of 0.42 and 0.51 in the CIE chromaticity diagram (Figure 2c). The results indicate the validity of 800 nm NIR light as the fluorescence light for excitation. Under continuous irradiation with high-power 800 nm (500 mW) NIR light, the yellow fluorescence of the BOSA-SP powders eventually changed to red fluorescence. Figure 2b shows that one distinct emission peak remained at 675 nm, with CIE coordinates of 0.63 and 0.37, whereas the emission peak at 526 nm greatly decreased, which suggested that high-power 800 nm NIR light successfully triggered the switch from BOSA-SP to BOSA-MC in the solid state. Therefore, BOSA-SP exhibited a third, rare, yellow fluorescence under excitation with 800 nm NIR light, which selectively switched to red fluorescence under the manipulation with high-power "trigger" light (800 nm).

To thoroughly investigate the relationship between the TPF intensity of BOSA-SP and the excitation power, the power-dependence of the TPF of the BOSA-SP powders was studied. We measured the TPF intensity of the emission band at 475–710 nm with an excitation wavelength of 800 nm (Figure S5). Figure S6 shows the dependence of the TPF intensity of the BOSA-SP powders on the incident light power intensity used for excitation. The fitted plots of the dependence of the fluorescence intensity on the pump light power intensity within 100–200 mW for the BOSA-SP powder showed good linear relationships with the slopes (1.99), which verifies that nonlinear TPF occurred after excitation with an 800 nm NIR laser.[11c,13] However, when the pump light power was higher than 200 mW, the emitted fluorescence began to deviate from the two-photon process. Speculatively, the following factors induced the deviation: 1) the relatively high pump light power could facilitate greater transformation from the SP to MC form, while local overheating of the confined focal plane by the NIR pump light causes reversion from the MC to SP form;[11c,13] and 2) more BOSA-MC in the powders may lead to intramolecular energy transfer from BOSA to the MC moiety, which could complicate the entire two-photon-excited transition process of BOSA-MC.[14]

"Pump" NIR light, which can excite the BOSA moiety effectively without inducing the photoisomerization of SP, was also examined. To this end, changes in the fluorescence spectrum of the BOSA-SP powders under irradiation with 950 nm NIR femtosecond light were investigated. Unlike the two emission peaks (526 nm and 671 nm) in the fluorescence spectrum under the irradiation with 800 nm light, the spectrum of the BOSA-SP powders (excitation: 950 nm) only exhibited an emission band at 525 nm (Figure S7a), which is consistent with the emission spectrum of the BOSA-SP powders under irradiation with 488 nm light (Figure S4a). Moreover, under continuous irradiation with 950 nm NIR light for 7 min, there was little fluctuation in the green fluorescence (emission: 525 nm) of the BOSA-SP powders (Figures S7b and S7c), which suggests that 950 nm NIR light should be effective as "pump" light for manipulating BOSA-SP to stably emit green fluorescence. Similarly, after BOSA-SP was continuously irradiated with 800 nm NIR light, a notable red emission peak centered at 662 nm appeared, indicating that the transformation of BOSA-SP to BOSA-MC was successfully triggered (Figure S7a), and reversible two-photon fluorescence switching was achieved after irradiation with the 524 nm light. Therefore, the fluorescence emitted from the photoexcited BOSA-SP can be selectively switched between green and red by irradiation with the "trigger" light (800/524 nm) after excitation with the "pump" NIR light (950 nm). Based on these results, we successfully manipulated BOSA-SP emission using multi-photon "pump-trigger" light, achieving stable fluorescence and programmable switching features, thereby enabling reversible solid-state three-color fluorescence switching.

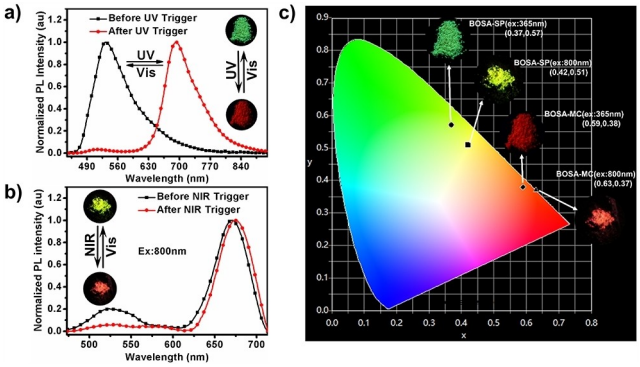

Figure 2. a) PL spectra of BOSA-SP powders before and after excitation with a 365 nm (UV) trigger light. The inset shows fluorescence images of BOSA-SP powders before and after irradiation with 365 nm light. b) PL spectra of BOSA-SP powders before and after irradiation with 800 nm (NIR) trigger light. The inset shows fluorescence images of the BOSA-SP powders before and after irradiation with 800 nm light. c) CIE chromaticity diagram with coordinates corresponding to the emission (365/800 nm) of BOSA-SP/MC powders.

Mechanism of Reversible Fluorescence Switching and Photoisomerization

To explore the mechanism of reversible fluorescence switching of BOSA-SP, the photophysical properties of SP and BOSA were investigated (Figure S9a and S9b). Compared with BOSA-SP, BOSA did not exhibit light-induced fluorescence switching properties (Figure S8), but exhibited similar photophysical properties in both powders and solution state (Figures 1b, 2a, S9a and S10). Moreover, there was no overlap between the absorption spectrum of SP and the emission spectrum of BOSA (Figure S9c), which indicated that there was likely no intramolecular energy transfer from BOSA to SP. Additionally, the central distance between the BOSA and SP moieties in the optimized geometry of the molecular structures of BOSA-SP was ≈1.47 nm (Figure S9e), which suggests that intramolecular charge transfer from BOSA to SP in BOSA-SP was unlikely. Thus, the green fluorescence of BOSA-SP was possibly from the BOSA moiety.[2c] The absorption and emission spectra of BOSA and BOSA-SP in different polar solvents were investigated, demonstrating that the absorption and emission peaks of the two molecules exhibited no obvious solvatochromic effect (Figure S11), which suggests that the emission of BOSA-SP was associated with the locally excited (LE) state of the BOSA moiety.[15] The natural transition orbital (NTO) of BOSA and BOSA-SP was further used to analyze the electron transition characteristics during emission. Figures 3b and S12 show that BOSA-SP and BOSA exhibited similar hole (the occupied orbital of the ejected electron) and particle (the virtual orbital at which the ejected electron is located) location on the BOSA moiety for the $S_1 \rightarrow S_0$ transition, which further confirms that the emission of the lowest singlet state (S_1) of BOSA-SP came from the LE state of the isolated BOSA moiety.[15b]

Aside from BOSA-SP, the absorption spectrum of the MC moiety of BOSA-MC substantially overlapped with the emission spectrum of BOSA moiety (Figure S9d), and the central distance between the BOSA and MC moieties in the optimized geometry of the molecular structure of BOSA-MC was ≈1.45 nm (Figure S9f).[16] These observations suggest that intramolecular energy transfer from BOSA to MC in BOSA-MC plausibly occurred,[2b,17] which possibly induced the fluorescence switching of BOSA-SP under irradiation with the "trigger" light. Analysis of the fluorescence lifetime showed that after the MC moiety was connected to BOSA, the fluorescence lifetime of BOSA decreased from 2.13 ns to 1.35 ns, which further suggests that intramolecular energy transfer occurred (Figure S13).[2c,14a] The NTO calculations for BOSA-MC show that the hole and particle involved in the $S_1 \rightarrow S_0$ transition in BOSA-MC were localized on the BOSA moiety, while they were localized on the MC moiety for the $S_2 \rightarrow S_0$ transition (Figures 3 and S14), which indicate that the green (weak) and red fluorescence of BOSA-MC came from the BOSA and MC moieties, respectively.[15b] As a result, the intramolecular energy transfer process from BOSA to MC weakens the green fluorescence from BOSA moiety on one hand, and enhances the red fluorescence from MC moiety on the other hand, leading to the switching from green to red fluorescence of the powders.

To explore the mechanism of reversible photoisomerization in the aggregated state, powder X-ray diffraction (PXRD) measurements of powdered BOSA-SP were performed before and after UV irradiation. Figure S15 shows that there were no obvious diffraction peaks in the XRD patterns of the powders in the different states, which means that the powdered BOSA-SP remained amorphous before and after it was triggered with UV light. To further explore the molecular conformation and packing of BOSA-SP in the aggregated state, molecular dynamics simulations were performed to predict molecular packing in the solid state.[2c,18] Figure S16a shows that BOSA-SP and BOSA-MC adopted a twisted molecular configuration and loose packing in the aggregated state, accounting for their amorphous structure. It is noteworthy that the single molecules of BOSA-SP and BOSA-MC occupied volumes of 66.35 ± 0.003 and 65.30 ± 0.002, respectively. Compared with the reported high volume of the SP (69.00 ± 0.21) and MC (67.60 ± 0.26) moieties,[2c] there was a significant reduction in the volume occupied by SP and its photoisomers (MC) after the twisted BOSA moiety was connected, which suggests that this connection created a large intermolecular space; the twisted BOSA moiety increased the intermolecular distance of the MC and SP moieties in the solid state, which enabled the "trigger" light to induce reversible reversion between MC and SP in the solid state.

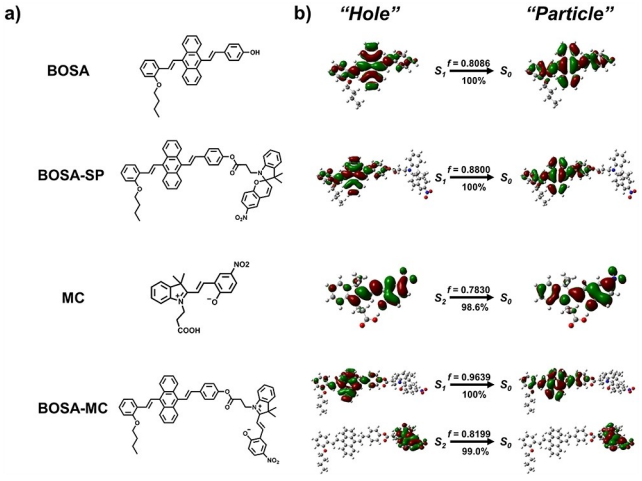

Figure 3. a) Molecular structures. b) The NTOs and oscillator strengths (*f*) for ($S_n \rightarrow S_0$, $n = 1$ or 2) the optimized geometric states of BOSA, BOSA-SP, MC, and BOSA-MC.

Multi-color Tunable Switching Cellular Imaging

We also explored the application of BOSA-SP in fluorescence-tunable bioimaging because of the novel solid-state controllable fluorescence switching properties of BOSA-SP. After encapsulating BOSA-SP in an amphiphilic polymer matrix, F127,[19] the one-pot self-assembly method was used to prepare BOSA-SP nanoparticles (NPs) (Fig-

ure S17a). The dynamic light scattering (DLS) and transmission electron microscopy (TEM) data (Figure S17b) show that the BOSA-SP NPs have a small average diameter of ≈37 nm. As expected, both the absorption and fluorescence spectra of the NPs exhibited similar fluorescence switching characteristics to those of powdered BOSA-SP (Figures S17c and S17d). After co-culturing HPV 18-positive cell line HeLa (ATCC) cells with the BOSA-SP NPs at different concentrations for 24 h, all the cells exhibited high viability (Figure S18), indicating that the BOSA-SP NPs had relatively low cytotoxicity. HeLa cells were then incubated with BOSA-SP NPs (50 μg mL^{-1}) for 2 h at 37 °C. Confocal laser scanning microscopy (CLSM) was used to monitor the fluorescence changes in the HeLa cells. The excitation wavelength and intensity of the green and red channels were fixed throughout the imaging process. Figure S19 shows that under constant illumination with "pump" light (488 nm), the incubated cells steadily fluoresced green (ex: 488 nm) in the green channel (490–600 nm) and faintly fluoresced red (ex: 594 nm) in the red channel (620–750 nm). Therefore, stable one-photon green fluorescence images were observed in the merged channel (Figure 4a). A similar experiment was then performed with "trigger" light (405 nm) to selectively switch the fluorescence of the incubated cells. Gradual abatement of fluorescence in the green channel and gradual intensification of fluorescence in the red channel were captured as the irradiation time elapsed. Eventually, the fluorescence of the cells with contrasting fluorescence gradually switched from green to red in the merged channel after 20 min of irradiation (Figure 4b). These findings further demonstrate the excellent controllable fluorescence output of BOSA-SP NPs and their viability as dual-color fluorescence dyes for bioimaging applications.

Based on the cellular imaging results from controllable OPF switching, we switched from illumination with 405 nm light to NIR light (800 nm) to explore TPF switching in cellular imaging applications. The same conditions for excitation (800 nm) were used for the green and red channels during imaging. Figure S21 shows that the cells incubated with BOSA-SP NPs notably fluoresced in the green (490–590 nm) and red channels (600–750 nm) under excitation with 800 nm light. Novel two-photon yellow fluorescence was also observed in the merged channel (Figure S21c), which is consistent with the TPF properties of powdered BOSA-SP. The intensity of the 800 nm light was then fixed and the incubated cells were continuously illuminated. Similar to the OPF switching, the fluorescence in the green channel gradually abated, whereas the fluorescence in the red channel gradually intensified (Figure S21) as the irradiation time increased. After approximately 20 min of illumination, NIR light was manipulated to successfully achieve unique two-photon dual-fluorescence switching from yellow to red for cellular imaging (Figure S21c). More importantly, merely by switching the wavelength of "pump" light, high-contrast cells fluorescence

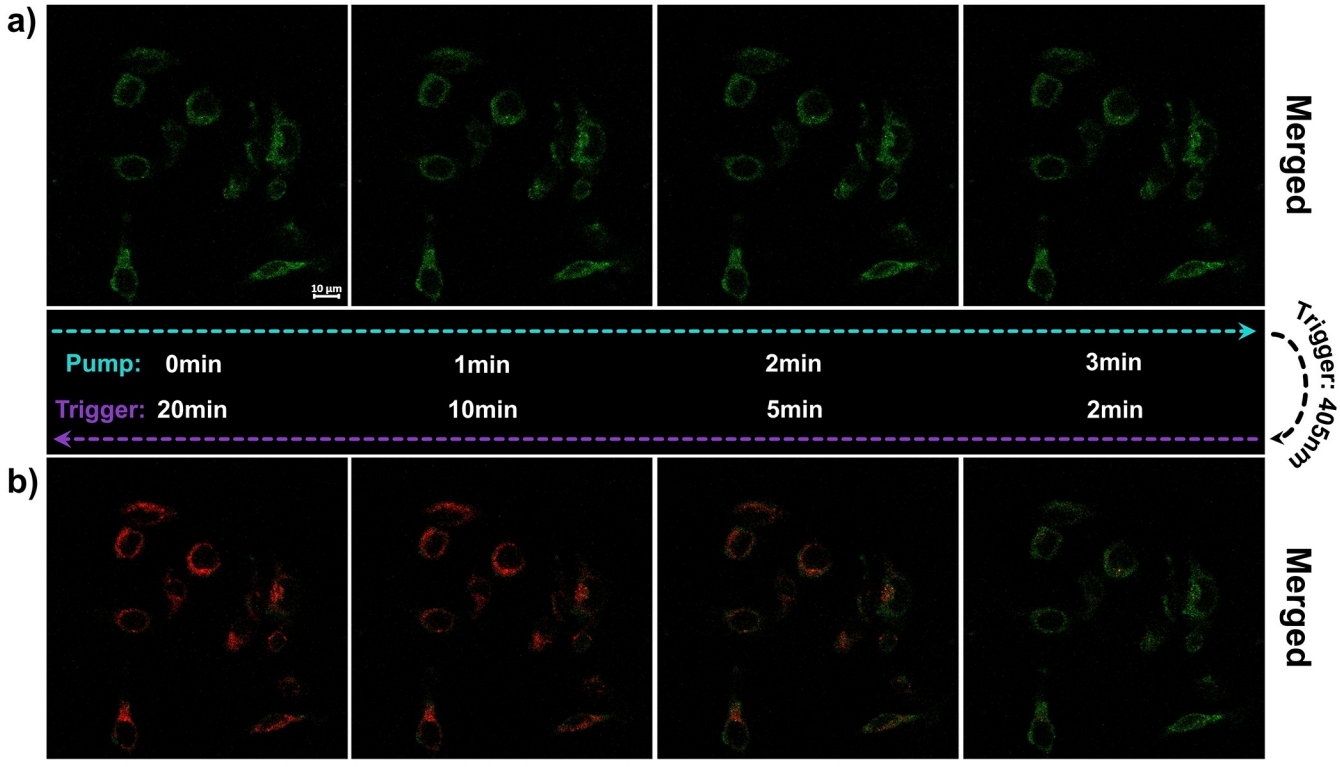

Figure 4. Time-dependent merged OPF confocal images of HeLa cells incubated with BOSA-SP NPs. a) Merged images of cells under continuous irradiation with "pump light (488 nm)" for 3 min. b) Merged images of cells under continuous irradiation of "trigger light (405 nm)" for 20 min. Scale bar = 10 μm.

switching (green-yellow) images were easily captured (Figure 5a and b). Additionally, when the "trigger" light (405/800 nm) and reversible "trigger" light (524 nm) were used to illuminate the original incubated cells during CLSM cellular imaging, two kinds of specific dual-fluorescence switching (green-red and yellow-red) were further captured (Figure 5). Based on these results, the confocal imaging of cells with programmable three fluorescence (green, yellow, and red) switching was successfully achieved (Figure 5), which greatly reduce cell autofluorescence interferences and provide high-contrast and legible cellular images. More importantly, because BOSA-SP is a single probe, it removes the need for consolidating different probes to achieve multi-fluorescence switching, and can be applied in super-resolution imaging fields.

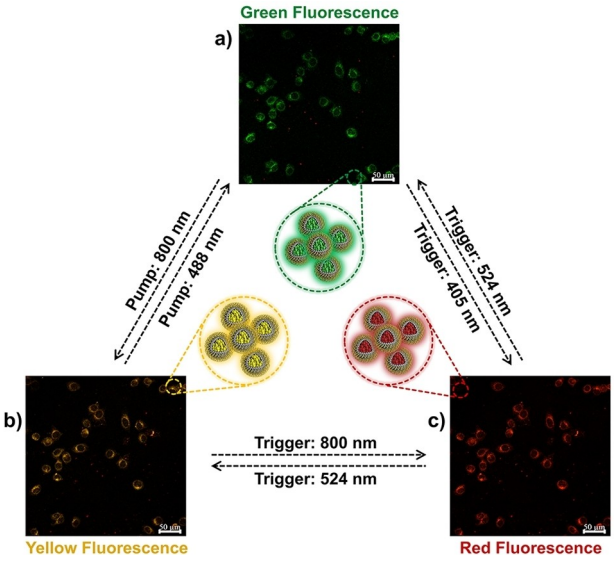

Figure 5. Merged triple fluorescence (green, yellow, and red) switching in the confocal images of HeLa cells incubated with BOSA-SP NPs under illumination at different wavelengths (excitation at a) 488 nm, b) 800 nm, and c) 800 nm). Scale bar = 50 μm.

Two-Color Super-Resolution Imaging

The solid-state dual-fluorescence switching properties of BOSA-SP inspired us to explore its unique applicability in the field of two-color super-resolution imaging. To achieve this goal, BOSA-SP was doped into diblock copolymer polystyrene-block-poly(ethylene oxide) (PSt-*b*-PEO) to self-assemble as cylindrical micelles (Figures 6a and b).[5k] Micelles with both green and red fluorescence (Figures 6c and d) were obtained by selecting different filters for imaging. Compared with the bright-field images, the fluorescence images acquired in a dark environment were more distinct, enabling accurate identification of the high-contrast micelles. However, the quality of the fluorescence images (Figures 6g and h) is limited by the optical diffraction of conventional microscopes, which resulted in a rough appearance of the morphology of the micelles, as evidenced by their blurry edges. Figures 6g and h also show that the micelles had a diameter of 524 nm in the green fluorescence image and 349 nm in the red fluorescence image. To reconstruct the two-color super-resolution images, the micelles were stained by continuous irradiation with 561 nm laser light and intermittent irradiation with 405 nm laser

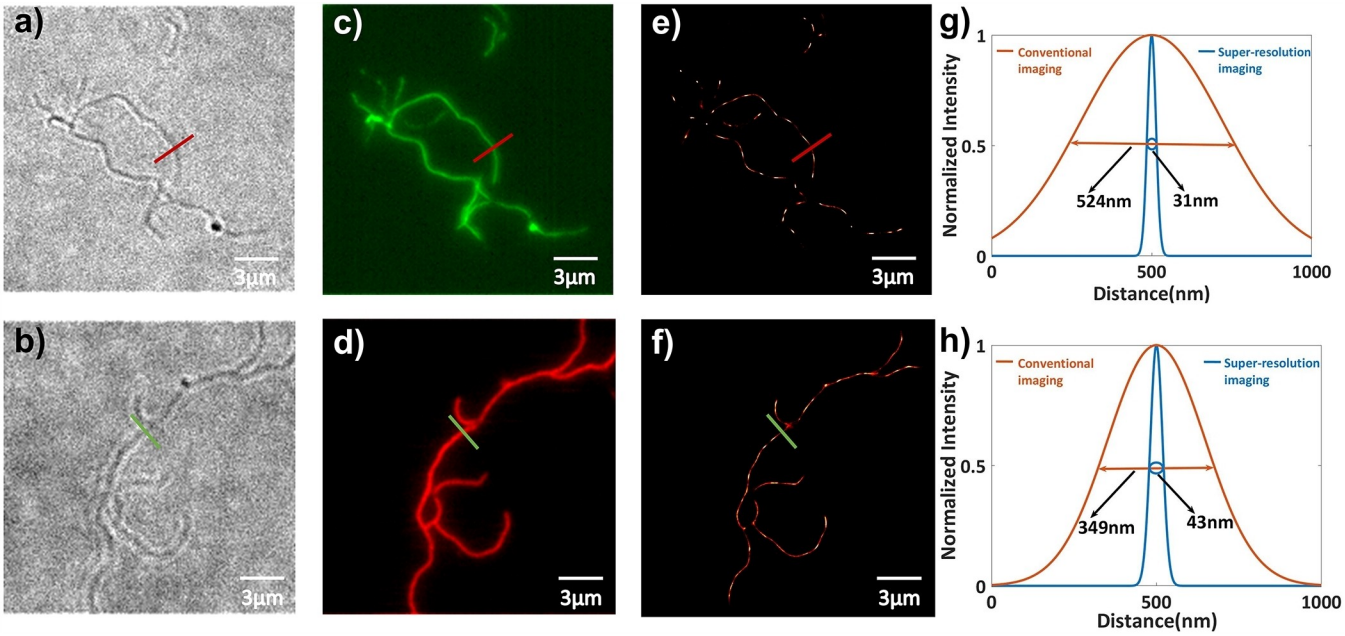

Figure 6. a) and b) Bright-field microscope images showing morphology of micelles. Conventional c) green and d) red fluorescence microscope images. Relative super-resolution imaging for e) green and f) red fluorescence. g) Green and h) red conventional fluorescence and super-resolution imaging of the cross-sectional profiles of the PSt-*b*-PEO cylindrical micelles at the dashed lines of the microscopy images.

light to regulate the two-color ON/OFF fluorescence switching of the BOSA-SP molecules. As shown in Figure 6e and f, novel two-color super-resolution imaging of the micelles was realized. Compared with the higher full width at half-maximum (FWHM) in conventional fluorescence imaging, the FWHM of super-resolution imaging, which greatly improved the quality of images, was calculated to be as low as 31 nm for green fluorescence and 43 nm for red fluorescence. The fluorescence quantum efficiency of the DSA derivate, BOSA, was notably high: the average photon numbers were 1213 for green fluorescence and 651 for red fluorescence (Figure S22a and S22b). Based on these values, further calculations using the Fourier ring correlation[20] showed that the overall resolution of the green fluorescence in super-resolution imaging was 46.43 ± 1.91 nm, which is better than 49.58 ± 2.39 nm for the red fluorescence (Figure S22c and S22d). Notably, BOSA-SP can innovatively achieve two color super-resolution imaging in one single molecular system. Furthermore, considering that the STORM super-resolution imaging quality is inseparable from the detected average photo number of fluorescent photoswitches, it allows us to further develop progressive super-resolution imaging technology that simultaneously collects multispectral photo numbers in both green and red fluorescence channels. The higher resolution and sharper images of STORM super-resolution imaging is therefore anticipated.

Conclusion

This study demonstrated the interesting solid-state fluorescence photoswitching of a novel spiropyran (SP)-functionalized distyrylanthracene derivative, BOSA-SP. More importantly, BOSA-SP was used to successfully achieve rarely observed triple fluorescence switching in a single system. To observe photoswitching, we used the "Pump–Trigger" strategy, in which the "pump" light (488/800/950 nm) induces photoluminescence and the "trigger" light (405/524/800 nm) activates reversible photoisomerization. This approach enables stable fluorescence and programmable switching in the aggregated state. Notably, such fluorescence switching is very efficient in the solid powders and nanoaggregates, which encouraged us to explore their potential application in advanced fluorescence microscopy. The present results show that using programmable "pump" and "trigger" lights in a single molecular system is suitable for in situ three-color tunable switching cell imaging and two-color super-resolution imaging. Thus, we envisage that this strategy may facilitate the development of multimodality fluorescence photoswitches and enrich the chemistry of photochromics. Furthermore, the stable dual fluorescence photoswitching feature is anticipated to improve the spatial resolution of super-resolution imaging, which increases the total photon number collected simultaneously from two channels of a single agent.

Acknowledgements

This work was supported by the Natural Science Foundation of China (21835001, 52073116, 51773080) and the JLU Science and Technology Innovative Research Team (2021TD-03).

Conflict of Interest

The authors declare no conflict of interest.

Data Availability Statement

The data that support the findings of this study are available in the Supporting Information of this article.

Keywords: Aggregation Regulation · Multi-Color Bioimaging · Photoswitches · Super-Resolution Imaging · Triple Fluorescence

[1] a) Y. Matsuo, K. Kanaizuka, K. Matsuo, Y.-W. Zhong, T. Nakae, E. Nakamura, *J. Am. Chem. Soc.* **2008**, *130*, 5016–5017; b) C. Jia, A. Migliore, N. Xin, S. Huang, J. Wang, Q. Yang, S. Wang, H. Chen, D. Wang, B. Feng, *Science* **2016**, *352*, 1443–1445; c) D. Kim, J. E. Kwon, S. Y. Park, *Adv. Funct. Mater.* **2018**, *28*, 1706213.

[2] a) M.-Q. Zhu, L. Zhu, J. J. Han, W. Wu, J. K. Hurst, A. D. Li, *J. Am. Chem. Soc.* **2006**, *128*, 4303–4309; b) Q. Qi, C. Li, X. Liu, S. Jiang, Z. Xu, R. Lee, M. Zhu, B. Xu, W. Tian, *J. Am. Chem. Soc.* **2017**, *139*, 16036–16039; c) R. Yang, Y. Jiao, B. Wang, B. Xu, W. Tian, *J. Phys. Chem. Lett.* **2021**, *12*, 1290–1294; d) Y. Jiao, R. Yang, Y. Luo, L. Liu, B. Xu, W. Tian, *CCS Chem.* **2022**, *4*, 132–140.

[3] a) L. Zhu, W. Wu, M.-Q. Zhu, J. J. Han, J. K. Hurst, A. D. Li, *J. Am. Chem. Soc.* **2007**, *129*, 3524–3526; b) Z. Tian, W. Wu, W. Wan, A. D. Li, *J. Am. Chem. Soc.* **2009**, *131*, 4245–4252; c) J. Wang, Y. Lv, W. Wan, X. Wang, A. D. Li, Z. Tian, *ACS Appl. Mater. Interfaces* **2016**, *8*, 4399–4406; d) X. Chai, H.-H. Han, A. C. Sedgwick, N. Li, Y. Zang, T. D. James, J. Zhang, X.-L. Hu, Y. Yu, Y. Li, *J. Am. Chem. Soc.* **2020**, *142*, 18005–18013.

[4] a) Q. Chen, D. Zhang, G. Zhang, X. Yang, Y. Feng, Q. Fan, D. Zhu, *Adv. Funct. Mater.* **2010**, *20*, 3244–3251; b) C. Li, W.-L. Gong, Z. Hu, M. P. Aldred, G.-F. Zhang, T. Chen, Z.-L. Huang, M.-Q. Zhu, *RSC Adv.* **2013**, *3*, 8967–8972; c) X. Li, C. Li, S. Wang, H. Dong, X. Ma, D. Cao, *Dyes Pigm.* **2017**, *142*, 481–490; d) S. Mo, Q. Meng, S. Wan, Z. Su, H. Yan, B. Z. Tang, M. Yin, *Adv. Funct. Mater.* **2017**, *27*, 1701210; e) Q. Yu, X. Su, T. Zhang, Y.-M. Zhang, M. Li, Y. Liu, S. X.-A. Zhang, *J. Mater. Chem. C* **2018**, *6*, 2113–2122; f) B. Fang, M. Chu, L. Tan, P. Li, Y. Hou, Y. Shi, Y. S. Zhao, M. Yin, *ACS Appl. Mater. Interfaces* **2019**, *11*, 38226–38231; g) T. Lin, X. Su, K. Wang, M. Li, H. Guo, L. Liu, B. Zou, Y.-M. Zhang, Y. Liu, S. X.-A. Zhang, *Mater. Chem. Front.* **2019**, *3*, 1052–1061; h) P. Q. Nhien, W.-L. Chou, T. T. K. Cuc, T. M. Khang, C.-H. Wu, N. Thirumalaivasan, B. T. B. Hue, J. I. Wu, S.-P. Wu, H.-C. Lin, *ACS Appl. Mater. Interfaces* **2020**, *12*, 10959–10972.

[5] a) J. W. Chung, S. J. Yoon, S. J. Lim, B. K. An, S. Y. Park, *Angew. Chem. Int. Ed.* **2009**, *48*, 7030–7034; *Angew. Chem.* **2009**, *121*, 7164–7168; b) L. Chen, J. Zhang, Q. Wang, L. Zou, *Dyes Pigm.* **2015**, *123*, 112–115; c) G. Sinawang, J. Wang, B.

Wu, X. Wang, Y. He, *RSC Adv.* **2016**, *6*, 12647–12651; d) H. Dong, M. Luo, S. Wang, X. Ma, *Dyes Pigm.* **2017**, *139*, 118–128; e) G. Liu, Y.-M. Zhang, L. Zhang, C. Wang, Y. Liu, *ACS Appl. Mater. Interfaces* **2018**, *10*, 12135–12140; f) Q. Luo, F. Cao, C. Xiong, Q. Dou, D.-H. Qu, *J. Org. Chem.* **2017**, *82*, 10960–10967; g) R. Singh, H.-Y. Wu, A. K. Dwivedi, A. Singh, C.-M. Lin, P. Raghunath, M.-C. Lin, T.-K. Wu, K.-H. Wei, H.-C. Lin, *J. Mater. Chem. C* **2017**, *5*, 9952–9962; h) L. Ma, S. Wang, C. Li, D. Cao, T. Li, X. Ma, *Chem. Commun.* **2018**, *54*, 2405–2408; i) J. Qi, C. Chen, X. Zhang, X. Hu, S. Ji, R. T. Kwok, J. W. Lam, D. Ding, B. Z. Tang, *Nat. Commun.* **2018**, *9*, 1848; j) N.-H. Xie, C. Fan, H. Ye, K. Xiong, C. Li, M.-Q. Zhu, *ACS Appl. Mater. Interfaces* **2019**, *11*, 23750–23756; k) C. Li, K. Xiong, Y. Chen, C. Fan, Y.-L. Wang, H. Ye, M.-Q. Zhu, *ACS Appl. Mater. Interfaces* **2020**, *12*, 27651–27662; l) L. Ma, C. Li, Q. Yan, S. Wang, W. Miao, D. Cao, *Chin. Chem. Lett.* **2020**, *31*, 361–364; m) H. Yang, M. Li, C. Li, Q. Luo, M. Q. Zhu, H. Tian, W. H. Zhu, *Angew. Chem. Int. Ed.* **2020**, *59*, 8560–8570; *Angew. Chem.* **2020**, *132*, 8638–8648.

[6] J. Walz, K. Ulrich, H. Port, H. C. Wolf, J. Wonner, F. Effenberger, *Chem. Phys. Lett.* **1993**, *213*, 321–324.

[7] G. Berkovic, V. Krongauz, V. Weiss, *Chem. Rev.* **2000**, *100*, 1741–1754.

[8] M. Natali, S. Giordani, *Chem. Soc. Rev.* **2012**, *41*, 4010–4029.

[9] a) N. Tamai, H. Miyasaka, *Chem. Rev.* **2000**, *100*, 1875–1890; b) H. Görner, *Phys. Chem. Chem. Phys.* **2001**, *3*, 416–423.

[10] F. M. Raymo, M. Tomasulo, *Chem. Soc. Rev.* **2005**, *34*, 327–336.

[11] a) M.-Q. Zhu, G.-F. Zhang, C. Li, M. P. Aldred, E. Chang, R. A. Drezek, A. D. Li, *J. Am. Chem. Soc.* **2011**, *133*, 365–372; b) L. Lin, Z. Zhang, Z. Lu, Y. Guo, M. Liu, *J. Phys. Chem. A* **2016**, *120*, 7859–7864; c) X. Liu, X. Jia, M. Fischer, Z. Huang, D. R. Smith, *Nano Lett.* **2018**, *18*, 6181–6187.

[12] a) Y.-X. Hu, X. Hao, L. Xu, X. Xie, B. Xiong, Z. Hu, H. Sun, G.-Q. Yin, X. Li, H. Peng, *J. Am. Chem. Soc.* **2020**, *142*, 6285–6294; b) Y. Zhao, X. Zhao, M. D. Li, Z. a Li, H. Peng, X. Xie, *Angew. Chem. Int. Ed.* **2020**, *59*, 10066–10072; *Angew. Chem.* **2020**, *132*, 10152–10158; c) H.-H. Fang, B. Xu, Q.-D. Chen, R. Ding, F.-P. Chen, J. Yang, R. Wang, W.-J. Tian, J. Feng, H.-Y. Wang, *IEEE J. Quantum Electron.* **2010**, *46*, 1775–1781; d) Y. Dong, B. Xu, J. Zhang, X. Tan, L. Wang, J. Chen, H. Lv, S. Wen, B. Li, L. Ye, *Angew. Chem. Int. Ed.* **2012**, *51*, 10782–10785; *Angew. Chem.* **2012**, *124*, 10940–10943; e) H. Wang, K. Ma, B. Xu, W. Tian, *Small* **2016**, *12*, 6613–6622; f) J. Zhang, S. Ma, H. Fang, B. Xu, H. Sun, I. Chan, W. Tian, *Mater. Chem. Front.* **2017**, *1*, 1422–1429; g) C. Qu, Z. Gao, Y. Chen, *J. Photochem. Photobiol. A* **2018**, *361*, 62–66.

[13] a) S. Wang, J. Liu, G. Feng, L. G. Ng, B. Liu, *Adv. Funct. Mater.* **2019**, *29*, 1808365; b) A. J. Raghavendra, W. E. Gregory, T. J. Slonecki, Y. Dong, I. Persaud, J. M. Brown, T. F. Bruce, R. Podila, *Int. J. Nanomed.* **2018**, *13*, 4283–4290; c) C. N. LaFratta, J. T. Fourkas, T. Baldacchini, R. A. Farrer, *Angew. Chem. Int. Ed.* **2007**, *46*, 6238–6258; *Angew. Chem.* **2007**, *119*, 6352–6374.

[14] a) F. Li, Z. He, M. Li, J. Zhang, J. Han, P. Lu, *Mater. Lett.* **2014**, *132*, 263–266; b) M. Li, F. Li, Z. He, J. Zhang, J. Han, P. Lu, *J. Appl. Phys.* **2014**, *116*, 233106.

[15] a) J. Zhang, B. Xu, J. Chen, L. Wang, W. Tian, *J. Phys. Chem. C* **2013**, *117*, 23117–23125; b) H. Liu, Q. Bai, L. Yao, H. Zhang, H. Xu, S. Zhang, W. Li, Y. Gao, J. Li, P. Lu, *Chem. Sci.* **2015**, *6*, 3797–3804; c) Q. Qi, J. Qian, X. Tan, J. Zhang, L. Wang, B. Xu, B. Zou, W. Tian, *Adv. Funct. Mater.* **2015**, *25*, 4005–4010.

[16] H. Wu, Y. Chen, Y. Liu, *Adv. Mater.* **2017**, *29*, 1605271.

[17] V. Dryza, E. J. Bieske, *J. Phys. Chem. C* **2015**, *119*, 14076–14084.

[18] D. Venkateshvaran, M. Nikolka, A. Sadhanala, V. Lemaur, M. Zelazny, M. Kepa, M. Hurhangee, A. J. Kronemeijer, V. Pecunia, I. Nasrallah, *Nature* **2014**, *515*, 384–388.

[19] L. Meng, S. Jiang, M. Song, F. Yan, W. Zhang, B. Xu, W. Tian, *ACS Appl. Mater. Interfaces* **2020**, *12*, 26842–26851.

[20] a) R. P. Nieuwenhuizen, K. A. Lidke, M. Bates, D. L. Puig, D. Grünwald, S. Stallinga, B. Rieger, *Nat. Methods* **2013**, *10*, 557–562; b) Y. Yokoyama, K. Nakatani, *Photon-working switches*, Springer, Heidelberg, **2017**, pp. 557–562.

Manuscript received: December 16, 2021
Accepted manuscript online: February 1, 2022
Version of record online: February 15, 2022